

Reconstruction of the trajectory of the Huygens probe using the Huygens Atmospheric Structure Instrument (HASI)

G. Colombatti^{a,*}, P. Withers^{b,c}, F. Ferri^a, A. Aboudan^a, A.J. Ball^c, C. Bettanini^a, V. Gaborit^d, A.M. Harri^e, B. Hathi^c, M.R. Leese^c, T. Mäkinen^e, P.L. Stoppato^f, M.C. Towner^c, J.C. Zarnecki^c, F. Angrilli^a, M. Fulchignoni^d

^aCISAS G. Colombo, University of Padova, Via Venezia 15, 35131 Padova, Italy

^bCenter for Space Physics, Boston University, 725 Commonwealth Avenue, Boston, MA 02215, USA

^cPlanetary and Space Sciences Research Institute, Centre for Earth, Planetary, Space and Astronomical Research, The Open University, Walton Hall, Milton Keynes MK7 6AA, UK

^dLESIA, Observatoire de Paris, 5 Place Janssen, 92195 Meudon, France

^eFinnish Meteorological Institute (FMI), Vuorikatu 15 A, 00100 Helsinki, Finland

^fMottMcDonald Ltd., London, UK

Received 29 June 2007; received in revised form 11 October 2007; accepted 13 November 2007

Available online 5 December 2007

Abstract

The Huygens probe returned scientific measurements from the atmosphere and surface of Titan on 14 January 2005. Knowledge of the trajectory of Huygens is necessary for scientific analysis of those measurements. We use measurements from the Huygens Atmospheric Structure Instrument (HASI) to reconstruct the trajectory of Huygens during its mission. The HASI Accelerometer subsystem measured the axial acceleration of the probe with errors of $3\text{E}-6\text{ m s}^{-2}$, the most accurate measurements ever made by an atmospheric structure instrument on another planetary body. The atmosphere was detected at an altitude of 1498 km. Measurements of the normal acceleration of the probe, which are important for determining the probe's attitude during hypersonic entry, were significantly less accurate and limited by transverse sensitivity of the piezo sensors. Peak acceleration of 121.2 m s^{-2} occurred at 234.9 km altitude. The parachute deployment sequence started at 157.1 km and a speed of 342.1 m s^{-1} . Direct measurements of pressure and temperature began shortly afterwards. The measured accelerations and equations of motion have been used to reconstruct the trajectory prior to parachute deployment. Measured pressures and temperatures, together with the equation of hydrostatic equilibrium and the equation of state, have been used to reconstruct the trajectory after parachute deployment. Uncertainties in the entry state of Huygens at the top of the atmosphere are significant, but can be reduced by requiring that the trajectory and atmospheric properties be continuous at parachute deployment.

© 2007 Elsevier Ltd. All rights reserved.

Keywords: Titan; Atmosphere; Huygens; Data reduction techniques; Atmospheric entry

1. Introduction

The European Space Agency's (ESA's) Huygens probe was designed to study the atmosphere and surface of Titan. Its objectives were to “carry out detailed in situ measurements of the physical properties, chemical composition, and dynamics of the atmosphere, and local characteriza-

tion of the surface” (Lebreton and Matson, 1997). Huygens was released from the Cassini spacecraft on 25 December 2004 and entered the atmosphere of Titan on 14 January 2005. The Cassini/Huygens mission has devoted significant resources to the exploration of Titan. The detailed measurements of Titan by the Huygens probe, made during a few hours and over a small area of Titan's surface, are complementary to the repeated and large-scale measurements of Titan by the Cassini orbiter (Lebreton and Matson, 1997, 2002; Lebreton et al., 2005).

*Corresponding author. Tel.: +39 049 8276848; fax: +39 049 8276855.
E-mail address: giacomo.colombatti@unipd.it (G. Colombatti).

The Huygens Atmospheric Structure Instrument (HASI), one of six scientific experiments on Huygens, is a multi-national package of sensors designed to measure the physical properties characterizing Titan's atmosphere (Fulchignoni et al., 1997, 2002, 2005). HASI's scientific goals were to determine the thermal structure of Titan's atmosphere, to characterize the electrical and acoustic environment, to identify the presence of condensates and clouds, to study atmospheric motions on all scales, and to infer physical and electrical properties of the surface. HASI's measurement objectives were to obtain profiles of atmospheric density, pressure, temperature, and conductivity and detect electromagnetic waves along the probe's trajectory. HASI contained four sensor packages, the accelerometers (ACC), the pressure profile instrument (PPI), the temperature sensors (TEM), and the permittivity, wave, and altimetry package (PWA). We shall not discuss the PWA results in this paper.

The Huygens mission timeline, which was extremely complex by the standards of previous entry probes, has been discussed by Lebreton et al. (2005) and we only summarize it here. Huygens was separated from Cassini by the Spin Eject Device, which was designed to accelerate Huygens to a speed of 33 cm s^{-1} with respect to Cassini and cause Huygens to rotate about its symmetry axis at about 7.5 rpm. NASA was responsible for delivering Huygens to the entry interface, an altitude of 1270 km above the surface of Titan, assumed to be a sphere of radius 2575 km. All altitudes in this paper are radial distances from the centre of mass of Titan minus 2575 km. Huygens was essentially dormant after its release from Cassini until 4 h and 24 min before its predicted arrival at the entry interface, at which time the probe power-on sequence began. Huygens entered Titan's atmosphere at a speed of 6 km s^{-1} and decelerated to 300 m s^{-1} within less than 5 min. At this time, around 157 km altitude, the first parachute deployment sequence started. This marked the end of the entry phase of the Huygens mission and the start of the descent phase. This time, t_0 , is an important event for Huygens and all Huygens measurements are referenced to it. It occurred at 09:10:20.828 UTC. The time t_0 occurred when the acceleration measured by the engineering Central Acceleration Sensor Unit (CASU) reached 10 m s^{-2} . Huygens deployed a series of parachutes after t_0 and the probe reached the surface of Titan 2 h 28 min after t_0 . All Huygens instruments made measurements after t_0 , but only HASI made measurements before t_0 . Huygens survived impact and operated for at least 3 h on the surface. Huygens data were received by Cassini from shortly after t_0 until Cassini set below the horizon of Huygens, over 1 h after impact.

The aim of this paper is to determine the trajectory of the Huygens probe within Titan's atmosphere using data collected by the HASI experiment. Knowledge of the trajectory of Huygens is necessary for scientific interpretation of the results of all Huygens instruments. We shall use data from the HASI ACC, PPI, and TEM sensors, as well

measurements of the mean molecular mass of Titan's atmosphere by the Huygens Gas Chromatograph–Mass Spectrometer (GC–MS) (Niemann et al., 2005).

2. Input data

The Huygens reference frame is defined in (Clausen et al., 2002).

The origin is located at the centre of the lower surface of the main platform of the Huygens probe. The $+X$ axis is along the probe's symmetry axis, pointing from the front nose cap to the back cover. The $+Z$ axis is perpendicular to the $+X$ axis and points from the origin towards the DISR (Descent Imager-Spectral Radiometer) instrument (Lebreton and Matson, 1997). The $+Y$ axis completes the right-handed set of axes. Huygens was designed such that the aerodynamic acceleration vector during the entry phase of the mission and the local vertical during the descent phase of the mission should have been along the X axis.

2.1. HASI ACC data

The HASI ACC subsystem included one single-axis servo accelerometer and three single-axis piezoresistive accelerometers. The servo accelerometer, known as the Xservo sensor, was aligned parallel to the probe's X axis. The axes of the three orthogonal piezoresistive accelerometers were along the probe's X , Y , and Z axes. They are called the Xpiezo, Ypiezo, and Zpiezo sensors, respectively.

2.1.1. HASI ACC Xservo data

Based on pre-flight calibration and in-flight checkouts prior to release from Cassini, the HASI ACC team predicted an instrument noise level on the order of $3\text{E}-6 \text{ m s}^{-2}$ and a zero offset of the order of $1\text{E}-4 \text{ m s}^{-2}$ (HASI ACC Data Processing and Calibration Report, HASI-RP-UPD-106). The HASI Xservo instrument was sampled at 400 Hz during the Huygens mission, but, due to bandwidth limitations, only every fourth data point was recorded, giving an effective sampling rate of 100 Hz. Each N , where N varied during the Huygens mission, of these values were summed onboard to reduce the sampling rate further (Table 1).

The Xservo instrument had two gain channels, high and low, and two amplification settings, fine and coarse, for a total of four operating modes. These modes control the nominal ranges and resolutions of the Xservo instrument, which are listed in Table 2 (Zarnecki et al., 2004).

Table 1
Sampling rate of Xservo instrument

Mission phase	N	Effective sampling rate (Hz)
Entry	32	3.125
Start of descent	24	4.167
End of descent	57	1.754

Table 2
HASI Xservo ranges and resolutions

Gain (G)	Amplification (A)	Range (m s^{-2})	Resolution (m s^{-2})
High (H)	Fine (F)	$\pm 20\text{E}-3$	$3\text{E}-6$
Low (L)	Fine (F)	$\pm 200\text{E}-3$	$30\text{E}-6$
High (H)	Coarse (C)	± 18.5	$3\text{E}-3$
Low (L)	Coarse (C)	± 185	$30\text{E}-3$

Table 3
Changes in Xservo gain and amplification during mission

Time w.r.t. t_0 (s)	Altitude (km)	Amplification	Gain
-543.375	–	F	H
-180.24	771.8	F	L
-154.55	634.5	F	H
-154.23	632.8	C	H
-107.23	386.3	C	L
-12.14	161.5	C	H
+4.165	155.8	C	L

The switching of the ACC Xservo mode is controlled via software by comparing the actual measurements with fixed threshold values during the entire Huygens mission. The initial mode was high gain and fine amplification. A timer changed the amplification to coarse a few seconds after t_0 , where it remained for the rest of the mission. Changes in gain and amplification during the mission are summarized in Table 3 (in this paper negative time is to be considered before t_0).

The Xservo sensor output is a voltage. The output voltage that corresponds to a specific acceleration depends on the Xservo gain and amplification. An average of N voltages can only be converted into an acceleration if all N measurements were made with the same gain and amplification, so one or two Xservo measurements around each change in gain or amplification are unreliable. Such measurements have been replaced by linear interpolations using neighbouring measurements.

The acceleration at the centre of mass of Huygens should be zero before atmospheric entry and the onset of atmospheric drag. However, observed pre-entry Xservo data display sinusoidal oscillations with a non-zero mean (Fig. 1).

2.1.2. HASI ACC Xpiezo, Ypiezo, and Zpiezo data

The three piezo sensors were designed to measure the large and rapidly varying deceleration of Huygens upon impact with the surface of Titan, not the large and slowly varying deceleration experienced along the X axis, nor the small decelerations experienced along the Y axis and Z axis, during the entry phase. The Xpiezo data are consistent with the Xservo data but have larger uncertainties, so we do not use the Xpiezo data in this study. The Ypiezo and Zpiezo sensors provided the only measurements of acceleration normal to the probe's symmetry axis during the entry phase.

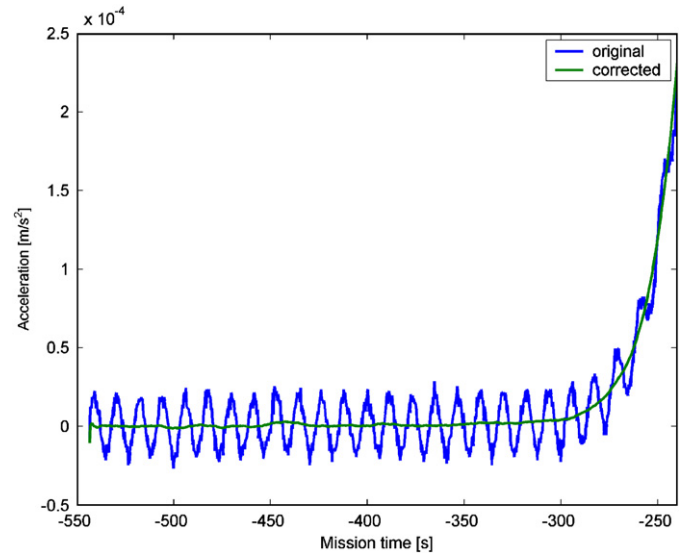


Fig. 1. HASI Xservo acceleration measurements from the start of the measurement sequence to atmospheric detection. The effective offset of zero- g has been estimated by the average of the Xservo data in the first 60 s window when the probe is still outside the onset of atmospheric drag. The zero- g offset is $2.2654\text{E}-4 \text{ m s}^{-2}$, which is the same order of magnitude of values estimated for in-flight CheckOuts (Zarnecki et al., 2004).

The resolution of the three piezo sensors was 0.24 m s^{-2} and their range was $\pm 200 \text{ m s}^{-2}$. Each sensor was sampled at 400 Hz, but only every eighth sample was recorded. Every block of 31 recorded samples was summed and transmitted to Cassini, giving an effective sampling rate of about 1.6 Hz. The range and resolution of the three piezo sensors were fixed. The zero offsets of the Xpiezo, Ypiezo, and Zpiezo instruments, based on analysis of their measurements before atmospheric entry (average values for the first 60 s) were 0.197 , 0.129 , and 1.228 m s^{-2} , respectively.

Ypiezo and Zpiezo readouts during Huygens probe entry are not significant except for the time of the deceleration peak. Since the piezo sensors are not perfect single-axis accelerometers they have a slight transverse sensitivity. In any case removing the transverse acceleration contribution from the Ypiezo and Zpiezo trace does not give any further information for trajectory reconstruction since the remaining values are below the resolution limit; piezos data elaboration are used only for boundaries of angle of attack determination.

2.2. Other accelerometer data

The Huygens probe contained several other engineering accelerometers, as well as a number of g -switches (Jones and Giovagnoli, 1997). The engineering CASU consisted of three single-axis accelerometers aligned parallel to the probe's symmetry axis, the X axis. CASU was designed to measure accelerations in the range of $0-98 \text{ m s}^{-2}$, was primarily used for triggering events during the entry, and has a sampling rate of 1 Hz. The peak deceleration

experienced by Huygens during entry exceeded CASU's range, so we do not use CASU measurements in this study.

The engineering Radial Acceleration Sensor Unit (RASU) consisted of two single-axis accelerometers designed to measure the probe's rotation about its symmetry axis within a range of 0–1.2 m s⁻². RASU data were not transmitted during the entry phase. Since reconstruction of the probe's attitude during the descent phase is not part of this study, we do not use the RASU data.

2.3. Huygens probe data

Several other inputs are needed in order to reconstruct the Huygens probe trajectory:

- the Aerodynamic database
- the CoM evolution
- the mass evolution

The Aerodynamic database used for this study is the one updated by the Prime Contractor for Huygens probe (Tran, 2005). The access to the probe database is controlled by the Knudsen number: for $Kn > 10$ the free molecular flow database is used; for $10 > Kn > 0.001$ the transitional flow is used and for $Kn < 0.001$ the continuum database is considered; furthermore the database also has values for the parachutes: the pilot, the main and the stabilizing parachutes.

The position of the Xservo seismic mass in the Huygens reference frame is $X = 69.44$ mm, $Y = 16.4$ mm, and $Z = 6.8$ mm. The ACC sensors were fixed in the Huygens reference frame, but the position of the centre of mass of Huygens in the Huygens reference frame changed during the mission. The CoM evolution has been provided by the Huygens Project.

During the entry phase, the mass of Huygens decreased due to (A) ablation of the front heatshield and (B) loss of the multi-layer insulation (MLI) that provided thermal protection during the 7-year cruise. During the descent phase, the mass of Huygens decreased due to the release of items such as the back cover, the main parachute, and the protection caps of the instruments. The heatshields were not instrumented, except for some temperature sensors on their internal faces, so the evolution of the heatshield mass during the entry phase is not known. The Prime Contractor for the Huygens probe has provided the Huygens Project with a model for the probe's mass loss during the entry phase:

$$m = m_0^{2\sigma(v_{\text{rel}}^2 - v_0^2)}, \quad (1)$$

where m is the probe mass, m_0 is the probe mass at the entry interface, σ is $4.18\text{E}-10 \text{ m}^2 \text{ s}^{-2}$, v_{rel} is the probe speed, and v_0 is the probe speed at the entry interface.

The probe's moment of inertia tensor, which is $I_{xx} = 127.97 \text{ kg m}^{-2}$, $I_{yy} = 75.85 \text{ kg m}^{-2}$, $I_{zz} = 71.9 \text{ kg m}^{-2}$, $I_{xy} = 0.45 \text{ kg m}^{-2}$, $I_{yz} = 0.338 \text{ kg m}^{-2}$, $I_{zx} = -0.096 \text{ kg m}^{-2}$

considered in this study was provided by the Huygens Project.

2.4. HASI ACC data processing

The pre-entry oscillations observed in the Xservo data can be fitted by

$$a_{\text{Xservo}}(t) = A + B \cos(2\pi f(t - t_0) + \varepsilon), \quad (2)$$

where $A = -2.2654\text{E}-5 \text{ m s}^{-2}$ is the zero- g offset, $B = 1.8\text{E}-5 \text{ m s}^{-2}$, $f = 0.085 \text{ Hz}$, and $\varepsilon \approx 1 \text{ rad}$. This period corresponds to 38 Xservo measurements.

Since the Xservo sensor is not at the centre of mass of Huygens, the instrument is sensitive to accelerations caused by the probe's angular velocity. These accelerations are a function of the probe's angular velocity and the displacement of the Xservo seismic mass from the probe's centre of mass.

Our analysis indicates that Huygens was coning prior to entry. Its angular velocity vector had a magnitude of $7.04 \pm 0.16 \text{ rpm}$ and was almost parallel to the probe's X axis (Goldstein, 1980). RASU data from the start of the descent phase indicate a probe rotation rate of 6.99 rpm, consistent with the expectation that the probe's rotation rate should not change during the entry phase.

This rotation rate is not coherent with the rotation rate determined by Cassini MAG (7.4 rpm) (Dougherty et al., 2005) and Attitude and Articulation Control Subsystem (8 rpm) immediately after Huygens probe release. It is not clear why the MAG and AACS values differ, but the evidence suggests that the probe spin slowed between release from Cassini and arrival at Titan. Investigations of this discrepancy are ongoing.

If we subtract Eq. (1) from the Xservo measurements, then the root-mean-square value of the pre-entry Xservo measurements is $3\text{E}-6 \text{ m s}^{-2}$, which is similar to the resolution and expected noise level (Zarnecki et al., 2004). However, this subtraction leaves residual fluctuations in acceleration which we wish to remove. We thus subtract in addition a 38-point running mean from the measurements. Since this correction reduces the vertical resolution of the HASI measurements and is unnecessary once the Xservo measurements greatly exceed $1.8\text{E}-5 \text{ m s}^{-2}$, we do not make any adjustments to the Xservo data after $t = -223.5 \text{ s}$.

Fig. 2 shows the original and corrected datasets around the time of atmospheric detection. The corrected acceleration increases exponentially with time after atmospheric detection, which is consistent with theoretical arguments. We define atmospheric detection to have occurred at the point where the corrected Xservo data equals the root-mean-square noise level. Atmospheric detection occurred at $t = -314.5 \text{ s}$ and 1498 km, 228 km above the official entry interface of 1270 km altitude. The peak acceleration profile of 121.2 m s^{-2} is visible in Fig. 3.

The Xservo measurements after t_0 are relatively complex to interpret, since the probe dynamics during the descent phase are more complicated than during the entry phase.

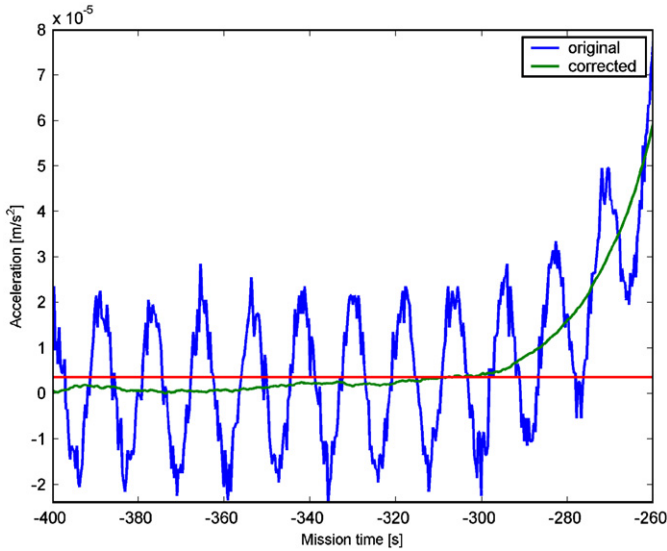


Fig. 2. Original and corrected Xservo measurements (m s^{-2}) versus time with reference to t_0 . The root-mean-square noise level is also shown (in red).

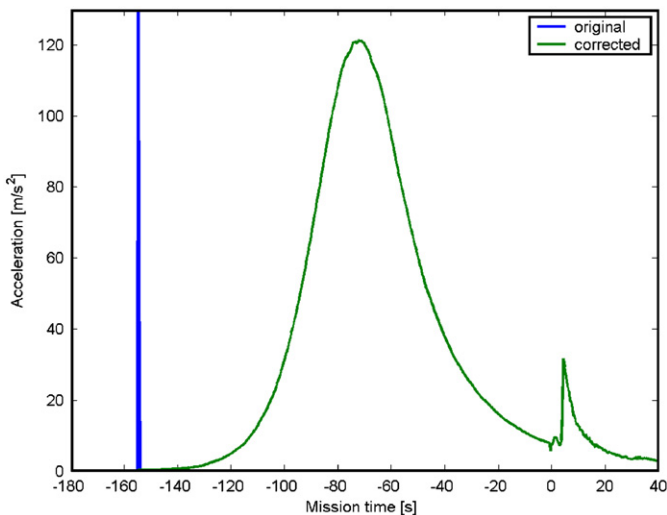


Fig. 3. Original and corrected Xservo measurements (m s^{-2}) versus time with reference to t_0 . Peak acceleration of 121.2 m s^{-2} occurred at $t = -72.4 \text{ s}$ and 234.9 km altitude. Pyro firing occur at t_0 and Main parachute deployment occurs at $t_0 + 2.5 \text{ s}$.

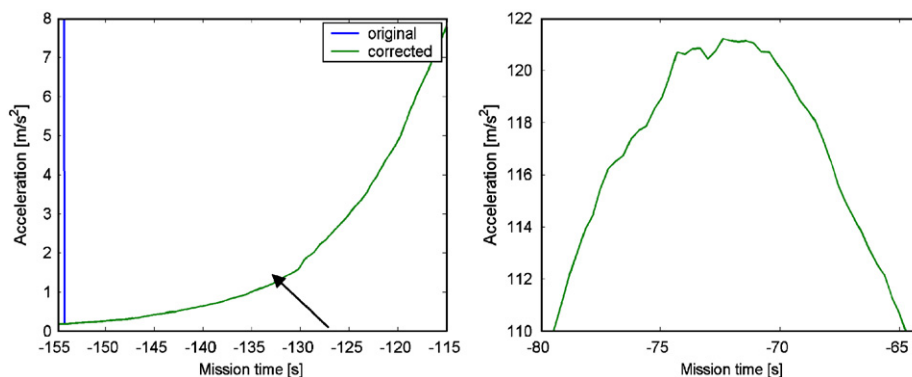


Fig. 4. Xservo measurements (m s^{-2}) versus time with reference to t_0 . On the left a slight bump in acceleration at -130 s is arrowed. On the right oscillations can be seen between about $t = -76 \text{ s}$ and $t = -68 \text{ s}$.

Events such as pyro firing and parachute deployment can be observed after t_0 . This time series of acceleration measurements is generally smooth before t_0 , but there are two notable exceptions. First, a slight bump is present around $t = -130 \text{ s}$, or 497 km (Fig. 4, left). Second, oscillations are present around peak deceleration, $t = -72.4 \text{ s}$, 232 km (Fig. 4, right). The slight bump around 500 km corresponds to the large temperature inversion at that altitude (Fulchignoni et al., 2005). Previous entry science experiments have not observed significant oscillations in acceleration around peak deceleration (Seiff and Kirk, 1977; Seiff et al., 1980, 1998; Spencer et al., 1999; Withers, 2006).

The presence of this oscillations seems to be related to atmospheric dynamics (e.g. tidal and or gravity waves; Strobel, 2006).

2.5. HASI PPI data

The PPI subsystem, which has direct access to the Titan atmosphere through a Kiel-type Pitot tube inlet, measures total (static plus dynamic) pressure (Mäkinen, 1996; Harri et al., 1998). It contains eight silicon capacitive absolute pressure sensors, known as Barocap sensors, which are divided into three groups based on the thickness of their silicon diaphragm. The thicker the diaphragm, the lower the resolution of the sensor. The ranges of the three groups are $0\text{--}400 \text{ hPa}$, $0\text{--}1200 \text{ hPa}$, and $0\text{--}1600 \text{ hPa}$. The absolute accuracy of each sensor is 1% of its range; the resolution of the sensors is $<0.04\%$ or $\pm 0.005 \text{ hPa}$. The Kiel probe inlet is mounted on a stem, known as the STUB, fixed to the external ring of the Huygens probe that is exposed to the atmosphere once the front heatshield is released.

The measured pressure, p_{meas} , does not equal the atmospheric pressure, p_{atm} , but the two are related (Doebelin, 1990) by

$$p_{\text{atm}} = p_{\text{meas}} \left(1 + \frac{\gamma - 1}{2} Ma^2 \right)^{\gamma/(1-\gamma)}, \quad (3)$$

where γ is the ratio of the specific heat capacity at constant pressure to the specific heat capacity at constant volume for

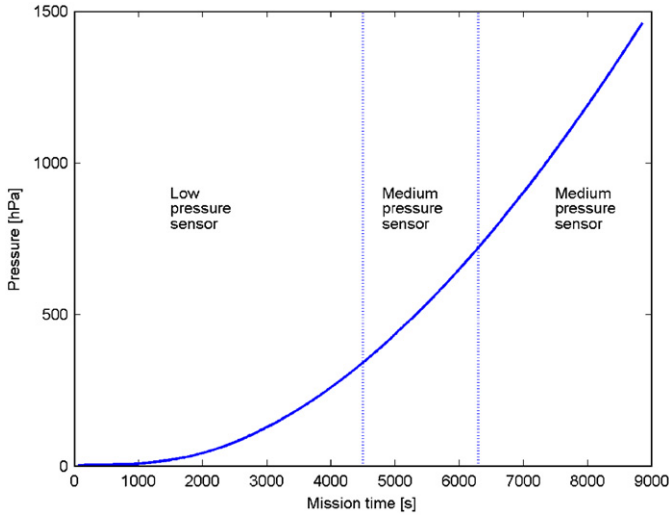


Fig. 5. Measured pressures (hPa) from PPI versus time after t_0 . The type of PPI sensor sampled changed during the descent phase as indicated.

the gas mixture and Ma is the Mach number of the flow. For small values of Ma , this equation reduces to $p_{\text{atm}} = p_{\text{meas}}(1 + \gamma Ma^2/2)$. Atmospheric pressure was derived from the measured total pressure through an iterative process that will be described in Section 3. PPI started collecting data at $t_0 + 10$ s and recorded two pressure measurements approximately every 2.3 s. Fig. 5 shows the time series of PPI measurements before correction for dynamic effects.

2.6. HASI TEM data

The HASI temperature sensors are dual element platinum resistance thermometers (Angrilli et al., 1996; Ruffino et al., 1996; Saggin et al., 1998). Each TEM unit comprises a primary, fine sensor, directly exposed to the airflow, and a secondary, coarse sensor, annealed into the supporting structure with a lower resolution. Two redundant pairs of fine and coarse sensors were mounted on the STUB. The TEM sensors have two gain states, high and low. The gain was switched from high to low when the measured temperature exceeded 105 K, and vice versa (Table 4).

One of the four TEM sensors was sampled every 1.25 s after $t_0 + 10$ s. The sampling sequence was fixed, so each TEM sensor was sampled every 5 s. The two coarse sensors were not sampled during the last kilometre of the descent and the sampling rate of each fine sensor was doubled from 0.2 to 0.4 Hz. Since all four sensors gave consistent results, we used only the measurements from the first fine (F1) sensor in this study.

The measured temperature, T_{meas} , does not equal the atmospheric temperature, T_{atm} , but the two are related (Doebelin, 1990) by

$$T_{\text{atm}} = \frac{T_{\text{meas}}}{1 + (rMa^2(\gamma - 1))/2}, \quad (4)$$

Table 4
TEM sensor characteristics

Gain state	Low (K)	High (K)
Range	90–330	60–110
Resolution	<0.07	<0.02
Accuracy (fine)	<2	<0.5
Accuracy (coarse)	<2	<0.8

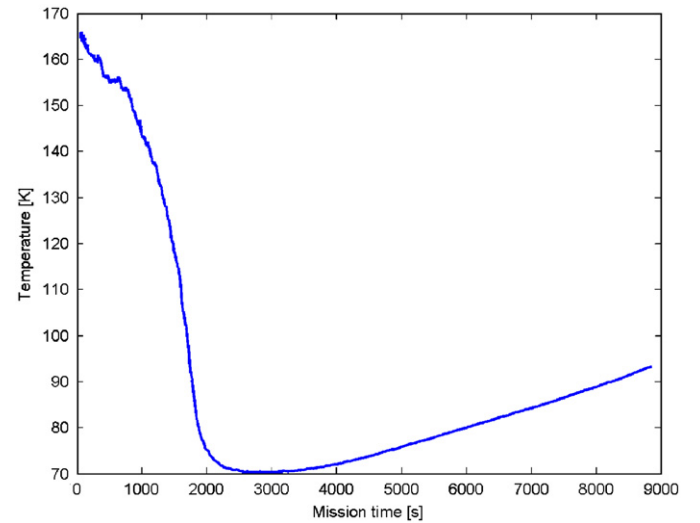


Fig. 6. Measured temperatures (K) from the TEM F1 sensor versus time after t_0 .

where r is a dimensionless recovery factor (assumed = 1), Ma is the Mach number of the flow, and γ is the ratio of the heat capacity at constant pressure to the heat capacity at constant volume for the gas mixture. Atmospheric temperature was derived from the measured temperature through an iterative process that will be described in Section 3. Fig. 6 shows the time series of TEM measurements before correction for dynamic effects.

2.7. Huygens GC–MS data

In order to retrieve a trajectory during the descent phase starting from pressure and temperature data the knowledge of atmospheric composition, specifically the mean molecular mass, μ , is required. The time series of the mixing ratios of CH_4 and N_2 (Titan's atmospheric major compounds) has been measured by the Huygens GC–MS experiment (Niemann et al., 2005).

3. Theory and methodology of trajectory reconstruction

During the entry phase, the probe was enclosed between the front and back heatshields for protection. During the descent phase, the probe was directly exposed to Titan's atmosphere. Since most Huygens instruments required exposure to the atmosphere to make useful measurements,

the only scientific instrument recording data during the entry phase was the HASI ACC sensors package. The front heatshield was released 32 s after t_0 , by which time PPI, TEM, and GC–MS had all started to record data. During the entry phase, Huygens was travelling at speeds significantly greater than the local speed of sound and simulations (Colombatti et al., 2008) allow to assume that the angle between the probe's symmetry axis and the velocity vector of the probe relative to the atmosphere, known as the angle of attack and labelled as α , was small, less than 4° . Furthermore, estimation of the AoA using the poor quality entry piezos data give boundaries for the AoA around $4/5^\circ$. During the descent phase, Huygens was descending slowly beneath a parachute and its dynamics and motion were significantly more complex than during entry. Since the dynamics of the probe differed significantly between these two parts of the mission we use different methodologies for the trajectory reconstruction.

3.1. Reconstruction methodology during the entry phase

The rates of change of position and velocity of the centre of mass of the Huygens probe during the entry phase satisfy the following equations:

$$\frac{d\vec{r}}{dt} = \vec{v} \quad (5)$$

$$\frac{d\vec{v}}{dt} = \vec{g} + \vec{a}_{\text{aero}}, \quad (6)$$

where \vec{r} is position, t is time, \vec{v} is velocity, \vec{g} is acceleration due to gravity, and \vec{a}_{aero} is aerodynamic acceleration.

HASI ACC measured the aerodynamic acceleration of Huygens during its entry and descent in a spacecraft-fixed reference frame. This can be transformed into the aerodynamic acceleration vector in a Titan-fixed reference frame using knowledge of the attitude of the Huygens probe. Since g is a function of position, these equations can be used to convert the time series of acceleration measurements into time series of velocity and position. Since Eqs. (5) and (6) are first-order differential equations, initial conditions for position and velocity are needed. The initial conditions used in this paper will be discussed in Section 3.3.

Accelerations measured in a Huygens-fixed frame must be converted into a Titan-fixed frame before they can be used in the trajectory reconstruction. An axisymmetric entry probe, such as Huygens, experiences accelerations parallel and perpendicular to its symmetry axis, a_A and a_N , respectively. These accelerations can be related to the accelerations parallel and perpendicular to the velocity of the probe relative to the atmosphere, a_D and a_L , respectively, as follows:

$$a_D = a_A \cos(\alpha) + a_N \sin(\alpha) \quad (7)$$

$$a_L = a_N \cos(\alpha) - a_A \sin(\alpha), \quad (8)$$

where α is the angle of attack. For Huygens, $a_A = a_X$ and $a_N = (a_Y^2 + a_Z^2)^{1/2}$. The direction of a_D , parallel to the velocity of the probe relative to the atmosphere, is known in a Titan-fixed frame, but the direction of a_L is not. However, the axisymmetric probe was designed such that α should remain small during the entry phase, so a_L should also be relatively small.

Furthermore, the pitching movement of the probe around the instantaneous velocity vector will drastically reduce the effect of any non-zero a_L on the trajectory. Therefore, we neglect a_L in the trajectory reconstruction. Determination of a_D from the measured a_A and a_N still requires knowledge of α . For a given entry vehicle, α is a single-valued function of the ratio a_N/a_A for fixed speed, atmospheric composition, density, and temperature. We used an iterative procedure and the atmospheric reconstruction results to determine α from a_N/a_A during the Huygens entry phase. Since the relationship between a_N/a_A and α is dependent on atmospheric composition, we used the Titan's atmosphere engineering model of Titan's atmosphere (Yelle, 2004) model to specify atmospheric composition at altitudes above those of the GC–MS measurements.

The angle of attack estimated from simulations is small ($<4^\circ$) (see Colombatti et al., 2008) and is used to access the Aerodynamic database in order to retrieve the aerodynamic coefficients during the reconstruction.

Sensitivity tests have been conducted using fixed AoA and no significant changes in trajectory reconstruction have been observed. It is therefore not significantly relevant if the considered AoA differs from zero (as done by the DTWG).

The gravitational acceleration at the position of Huygens was calculated using a spherically symmetric Titan of mass $1.3455E23$ kg and radius 2575 km. The atmosphere relative velocity, v_{rel} , is affected by winds. A Titan zonal wind model was used to specify the wind during the entry phase (Flasar et al., 1997).

The entry reconstruction was performed in a frame of reference that rotated at Titan's angular velocity using a Runge-Kutta–Fehlberg seventh-order integration method using similar methodology used in previous reentry probe missions (Seiff et al., 1998; Spencer et al., 1999; Withers et al., 2003, 2004; Gaborit, 2004; Withers, 2006).

Entry phase reconstruction stops at $t_0 + 32$ s when the front shield is released.

3.2. Descent reconstruction methodology

Atmospheric pressure satisfies the equation of hydrostatic equilibrium:

$$\frac{dp}{dr} > \rho g_r, \quad (9)$$

where p is atmospheric pressure, ρ is atmospheric density, r is distance from the centre of mass of Titan, and g_r is the radial component of Titan's gravitational acceleration,

including Coriolis and centrifugal terms. Atmospheric pressure p , temperature T , and density ρ on Titan are linked together by the equation of state of a real gas:

$$\frac{p\mu}{\rho RT} = 1 + B_2(\mu, T) \frac{\rho}{\mu}, \quad (10)$$

where R is the universal gas constant, μ is the mean molecular mass of the atmosphere, and $B_2(\mu, T)$ is the second virial coefficient of the gas mixture, given by

$$B_2 = 10^{-6} f^2 (-4 - 56X - 12X^2) \quad (11)$$

$$X = \frac{T}{298.15 \text{ K}} - 1, \quad (12)$$

where f is the fraction of atmospheric molecules that are molecular nitrogen (see Harri et al., 2006 for a more complete presentation). If we assume that Titan's atmosphere is a mixture of CH_4 and N_2 , then:

$$\mu = 28f + 16(1 - f). \quad (13)$$

HASI PPI and TEM measurements were corrected for dynamical effects using an iterative process. GC–MS measurements of mixing ratios were used to determine f and corrected HASI temperature measurements were used to determine X . B_2 was then calculated from f and X . Next, Eq. (10) was used to determine ρ from μ , B_2 , p , and T .

The equation of hydrostatic equilibrium can be combined with the equation of state to obtain:

$$\frac{RT}{\mu g_r} \left(1 + \frac{B_2 \rho}{\mu} \right) \frac{d \ln p}{dt} = \frac{dr}{dt} \quad (14)$$

All quantities on the left side of Eq. (14) can be determined from HASI and GC–MS measurements, except g_r , which is a known function of r . We used this first-order differential equation to reconstruct the altitude of Huygens during the descent phase. In contrast to the entry phase reconstruction, where we used initial conditions at the top of the atmosphere to solve the appropriate differential Eqs. (5) and (6), for descent phase reconstruction we used initial conditions at surface level (altitude = 0 m; vertical velocity = -4.5 m s^{-1}) and integrated equations upward. We assumed that the altitude of the impact site above the reference 2575 km radius sphere was zero and found that the vertical speed at impact was -4.5 m s^{-1} (positive upwards) (Zarnecki et al., 2005). Cassini RADAR and Huygens DISR observations suggest that Titan's surface contains little topographic relief, so our assumed impact

altitude of 0 km should be accurate to less than 1 km (Elachi et al., 2005; Tomasko et al., 2005). The descent phase reconstruction stops at $t_1 = t_0 + 60.544 \text{ s}$.

3.3. Determination of the Huygens entry state

The position and velocity of Huygens at a given time at the top of the atmosphere are very uncertain. This introduces substantial uncertainties into the reconstructed trajectory.

We reconstructed the entry phase trajectory forwards in time from initial conditions at the top of the atmosphere until $t_0 + 32 \text{ s}$. Independently, we reconstructed the descent phase trajectory backwards in time from the surface of Titan until t_1 , starting from an assumed altitude of 0 km at the surface. Clearly, the reconstructed trajectories and profiles of atmospheric properties must be consistent at t_0 ; there is a gap of about 30 s between the two reconstructions. This is due to the aerodynamic instabilities that occur after the front shield release and that do not allow us to use pressure and temperature data before t_1 .

The entry phase trajectory reconstruction requires an initial vector position and vector velocity, collectively known as an entry state. This entry state has a significant influence on the reconstructed trajectory. Cassini Navigation Team (CNT) analysis of radio tracking of Cassini, together with modelling of the Huygens release process and Cassini imaging of the Huygens probe 1–2 days after release, has determined an entry state (time, position, velocity) for Huygens at the Titan entry interface, fixed at 1270 km. However, due to the 3-week interval between the release of Huygens and its arrival at Titan, uncertainties in the entry state are significant.

HASI started to operate and detected the atmosphere above the official entry interface of 1270 km. Therefore, we began our trajectory reconstruction at 1531 km, before HASI's detection of the atmosphere. A nominal Huygens entry state at 1531 km, has been obtained by propagating the probe's trajectory upwards from the CNT-derived entry state at 1270 km altitude to 1531 km (from JPL-050214 DELIVERY) (Table 5).

There are several constraints that our reconstructed trajectory must satisfy: impact, detected by the measurements of the three HASI piezo accelerometers, should occur at an altitude of 0 km; vertical speed, density, pressure and temperature should be continuous at t_0 .

Table 5
Cassini Navigation Team-derived entry states at 1270 and 1531 km

Entry point	Interface time	Altitude (km)	Velocity (m s^{-1})	Flight path angle ($^\circ$)	Flight azimuth angle ($^\circ$)	Latitude ($^\circ$)	Longitude ($^\circ$)
Nominal	14 January 2005, 09:05:52.5226	1270.011 \pm 32	6031.239 \pm 3.5	65.4 \pm 0.3	259.897	−8.5	185.53
Higher	14 January 2005, 09:05:00.0000	1531.2	6006.6	67.05	260.144	−8.268	176.356

Uncertainties for the Higher entry point are consistent with the uncertainties at the Nominal entry point.

Table 6
The HASI entry state

Altitude (km)	Velocity (m s^{-1})	Flight path angle ($^{\circ}$)	Flight path azimuth ($^{\circ}$)	Initial pressure (Pa)	Latitude ($^{\circ}$)	Longitude ($^{\circ}$)
1531.2	6006.6	67.05	260.144	7.39409E-08	-8.268	176.356

Table 7
The Nominal entry state adjusted with HASI entry state

Altitude (km)	Velocity (m s^{-1})	Flight path angle ($^{\circ}$)	Flight path azimuth ($^{\circ}$)	Initial pressure (Pa)	Latitude ($^{\circ}$)	Longitude ($^{\circ}$)
1249.7	6034.0	65.35	259.897	2.50882E-06	-8.606	174.531

Although not discussed in this work, atmospheric density, pressure, and temperature profiles have been determined for the entry phase of the Huygens mission from HASI data (Fulchignoni et al., 2005).

We began with this entry state at 1531 km, reconstructed the Huygens trajectory, and tested whether the reconstructed trajectory satisfied the constraints adequately. Using a process of varying initial position and velocity vectors inside the uncertainties given by CNT and checking which where the minimum residuals in the region 155–145 km between the obtained physical entry profiles (density, pressure and temperature) and a polynomial interpolation of the same physical descent profiles, we reconstructed the trajectory with similar, but different, entry states until the reconstructed trajectory did satisfy the above constrains constraints adequately.

Our reconstructed position and velocity at 1270 km differs from the JPL-derived entry state. The corresponding altitude change is consistent with the uncertainties in the CNT entry state (Table 6).

This entry state corresponds to the following parameters at the Nominal interface time (Table 7).

Standard SPICE tools can be used to convert the reconstructed position and velocity into other frames (i.e. EME2000) and values are not here presented.

4. Results of trajectory reconstruction

The results of the trajectory reconstruction are shown in Figs. 7–12. An initial increase in the probe's speed after atmospheric entry can be seen in Fig. 8, corresponding to the continuing gravitational pull of Titan on Huygens. The Titan wind model predicts zonal wind speeds $\sim 100 \text{ m s}^{-1}$ during the entry phase (Flasar et al., 1997). The probe decelerated from 6 km s^{-1} at entry to $\sim 300 \text{ m s}^{-1}$ at t_0 , so differences between the actual wind speed and the predicted wind speed could cause errors in the reconstructed trajectory shortly before t_0 . Substantial horizontal motion of the probe can be seen between atmospheric entry and t_0 . This should be considered when the HASI atmospheric structure results are interpreted (Fulchignoni et al., 2005). Determination of the attitude of Huygens,

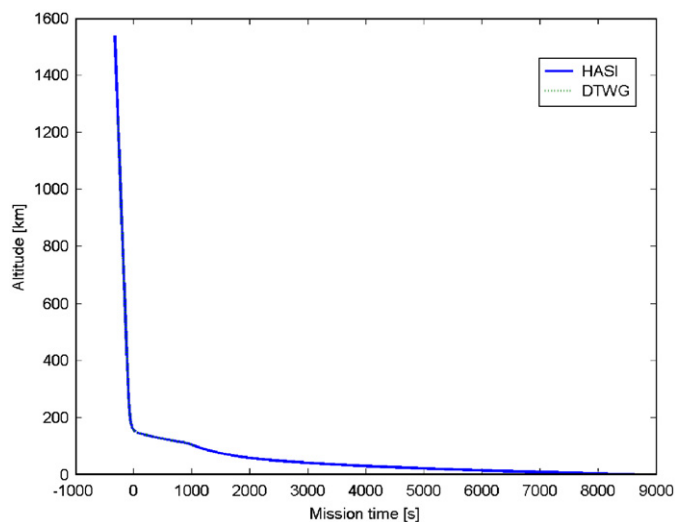


Fig. 7. Reconstructed altitude (km) versus time with reference to t_0 for the entry and descent phases. Both HASI and DTWG are plotted; difference in altitude is small and well inside the boundary of uncertainties of the two reconstructions.

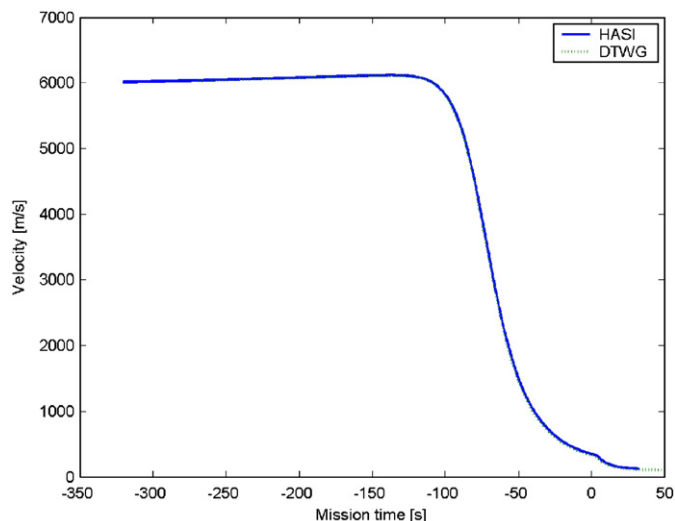


Fig. 8. Speed (m s^{-1}) versus time with reference to t_0 for the entry phase.

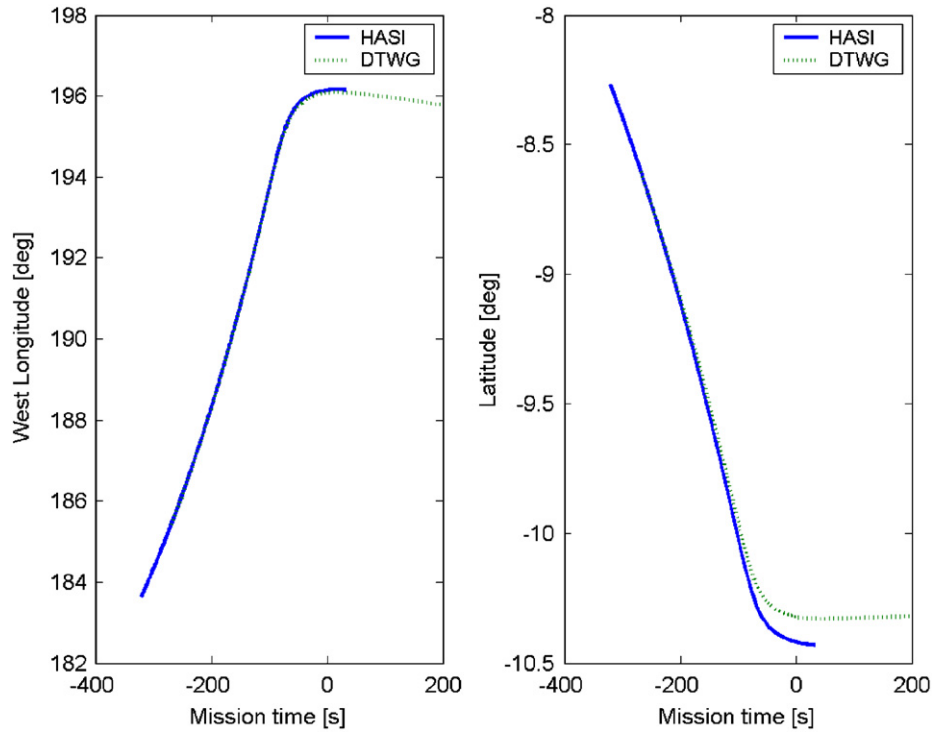


Fig. 9. Evolution of longitude (°W) and latitude (°N) during entry phase with reference to t_0 for the entry phase. HASI and DTWG profiles differ because of the different entry vector selected in the two reconstructions.

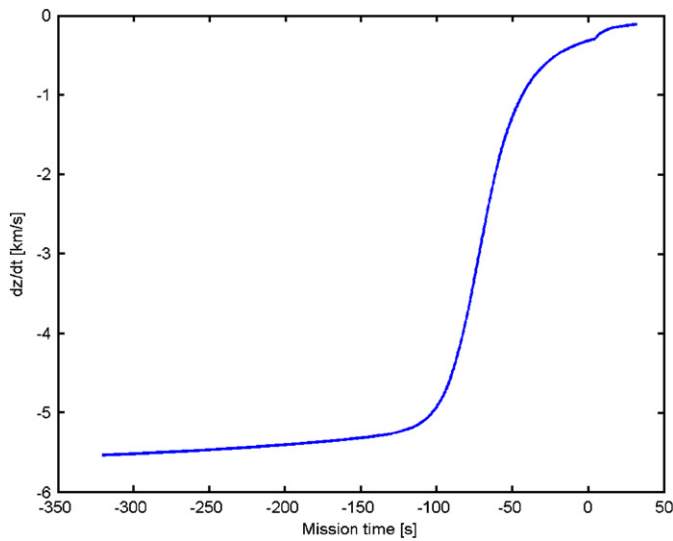


Fig. 10. Rate of change of altitude (km s^{-1}) with reference to t_0 for the entry phase.

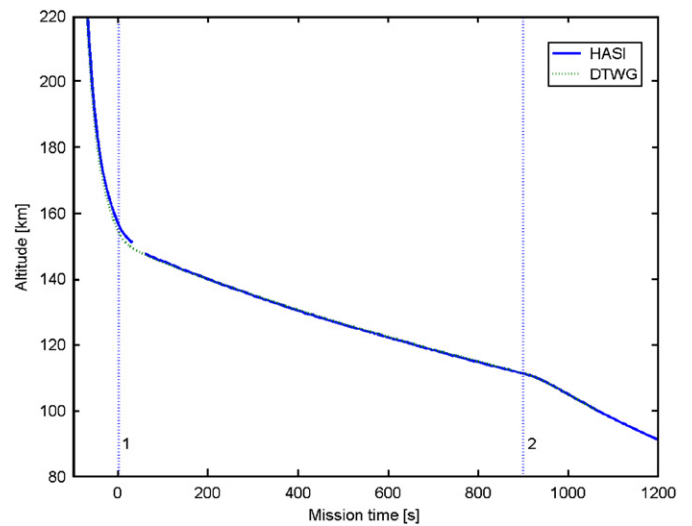


Fig. 11. Altitude (km) with reference to t_0 expanded from Fig. 7. This time interval spans the deployment of the main (line 1) and drogue (line 2) parachutes.

specifically its angle of attack, during the entry phase is an important part of the trajectory reconstruction process. Large errors in the angle of attack can have significant effects on the reconstructed trajectory and atmospheric structure. Although the HASI ACC Y and Z sensors were not optimized for this task, their measurements give information on the upper boundary of the probe’s angle of attack ($<4^\circ$) during the entry phase (Table 8).

We have adjusted the entry state to maximize the continuity of rate of change of altitude, density, pressure, and temperature from the entry phase to the descent phase at t_0 . Recall that Fig. 11 showed a discontinuity of about 1 km in altitude in the window $[t_0 + 30t_0 + 60]$ s. Although there is a gap of about 10 km the density, pressure and temperature profiles are continuous (Figs. 13 and 14).

5. Uncertainties in reconstructed trajectory

Sources of error in the entry phase of the reconstructed trajectory include:

- errors in the entry state;
- measurement errors in the measured Xservo accelerations;
- apparent acceleration due to displacement of sensor w.r.t. CoM;
- uncertainty in the knowledge of the angle of attack as derived from HASI ACC measurements w.r.t. Huygens experienced angle of attack;
- errors due to neglecting Saturn's gravitational field and the non-spherically symmetric components of Titan's gravitational field;
- errors in the direction of \vec{v}_{rel} due to winds in Titan's atmosphere;
- uncertainties in Huygens probe parameters: errors in the Inertia Matrix the mass and the dimensions; errors in the Aerodynamic database;
- the finite time interval between measurements, which leads to numerical error.

We have performed sensitivity tests to study the effects of several of these sources of error on the reconstructed trajectory.

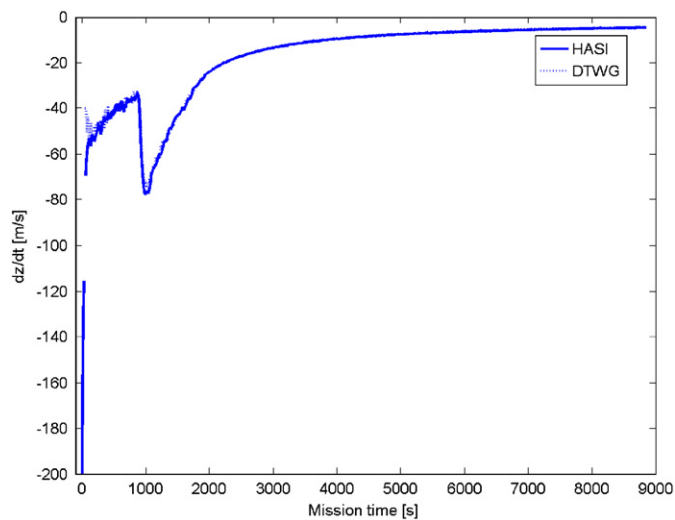


Fig. 12. Rate of change of altitude (m s^{-1}) versus time after t_0 (left line values for entry phase; right line values for descent phase: a 10 points smoothing has been applied on the descent phase altitude rate of change). Gap between the two lines is the window $t_0 + 32 \text{ s} - t_0 + 60.544 \text{ s}$ where data are missing.

Effects of changes in speed (v), altitude (Z), and flight path angle (FPA) at the time of entry upon conditions at t_0 have been investigated, keeping fixed two parameters and changing the third one by $\pm 1\sigma$ (see Table 9).

The velocity at t_0 is relatively insensitive to errors in the entry state at the top of the atmosphere. The difference between the altitude at the time of entry and the altitude at t_0 is sensitive to the altitude at the time of entry (up to 51 km for $Z = 1590 \text{ km}$), so the altitude at t_0 , based on the entry phase reconstruction, is quite uncertain. The altitude of t_0 is also quite sensitive to the FPA at entry (around 6 km). However, the requirement that the descent phase reconstruction starts at t_0 and ends at impact on the surface of Titan means that the actual uncertainty in the altitude of t_0 is less than that suggested by the above sensitivity tests. Conditions at t_0 are extremely sensitive to any systematic error in the Xservo data. Altitude and velocity have been reconstructed using nominal ACC Xservo data and also considering Xservo $\pm 1\sigma$. While altitude variations at t_0 are respectively less than 4 km the velocity variations are around 50 m s^{-1} (corresponding to 15% of nominal value); this is probably due to incorrect modelling of the Huygens probe dynamics between t_0 and $t_0 + 32 \text{ s}$ when the parachute deployment sequence starts. Thus, accurate knowledge of the zero offset of the Xservo instrument is critical for a successful trajectory reconstruction. If the actual angle of attack and the reconstructed angle of attack are both small, on the order of less than 4° , then the

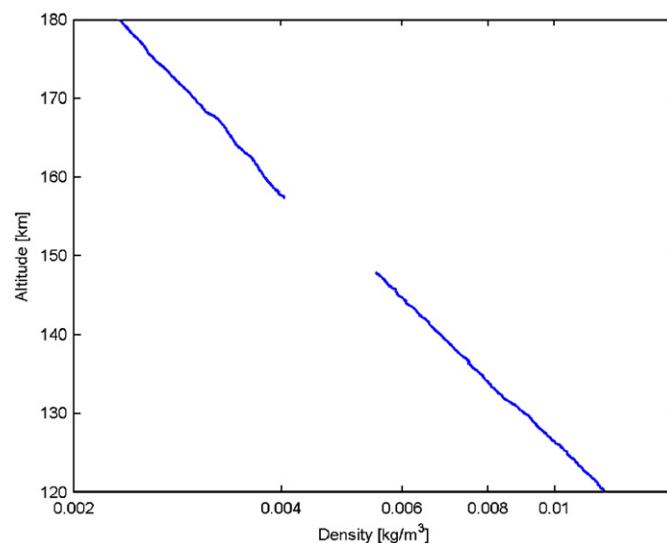


Fig. 13. Density (kg m^{-3}) versus altitude (km) around t_0 (gap between the two lines is the window $t_0 + 32 \text{ s} - t_0 + 60.544 \text{ s}$ where data are missing).

Table 8

Conditions at beginning of descent phase (t_0) and impact

	Mission time respect t_0 (s)	UTC time	Altitude (km)	Velocity (m s^{-1})
Start of descent	+0	9:10:20.828	157.1	-342.1
Impact	+8869.875	11:38:10.703	0	-4.5

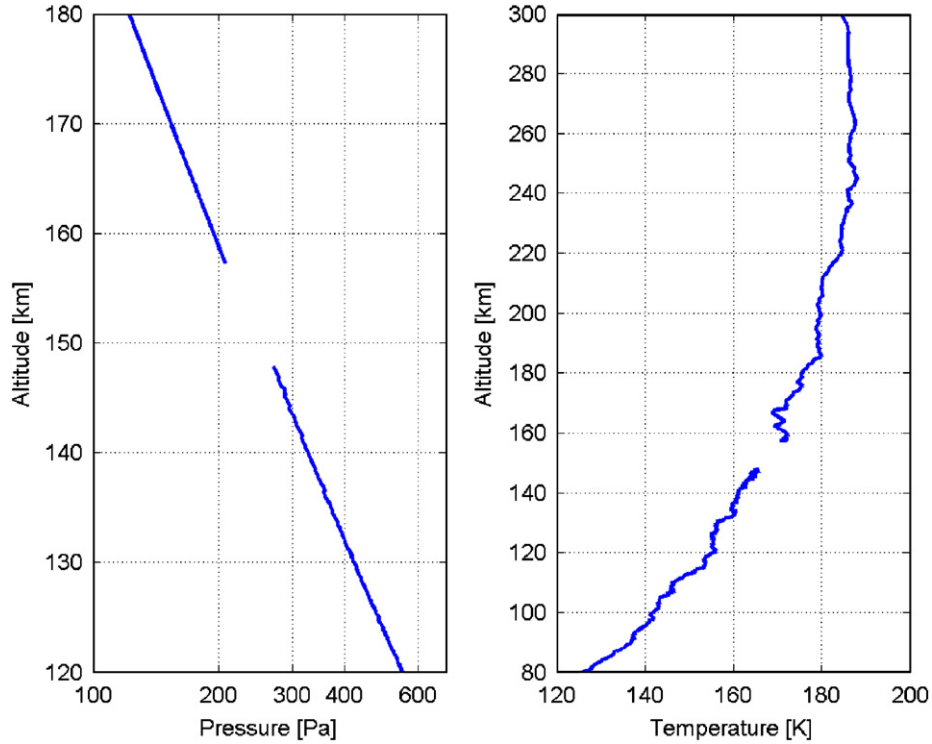


Fig. 14. Pressure (Pa) and temperature (K) versus altitude (km) around t_0 (gap between the two lines is the window $t_0 + 32$ – $t_0 + 60.544$ s where data are missing)..

Table 9
Effects of changes in speed (v), altitude (Z), and flight path angle (FPA) at the time of entry upon conditions at t_0

Fixed parameters	Variable parameter	Altitude at t_0 (km)	Velocity at t_0 (m s^{-1})
$v = 6006.6 \text{ m/s}$, FPA = 67.05°	$Z = 1531 \text{ km}$	157.1	342.1
	$Z = 1570 \text{ km}$	189.0	337
	$Z = 1590 \text{ km}$	208.9	334.6
$Z = 1531.2 \text{ km}$, FPA = 67.05°	$v = 5999.6 \text{ m s}^{-1}$	158.9	335.3
	$v = 6003.1 \text{ m s}^{-1}$	158.0	338.7
	$v = 6006.6 \text{ m s}^{-1}$	157.1	342.1
$Z = 1531.2 \text{ km}$, $v = 6006.6 \text{ m s}^{-1}$	FPA = 66.95°	158.7	341.6
	FPA = 67.05°	157.1	342.1
	FPA = 67.35°	152.4	343.6

reconstructed conditions at t_0 are relatively insensitive to errors in the angle of attack. However, if the actual angle of attack were $\sim 7^\circ$ and the reconstructed angle of attack were $\sim 2^\circ$, then the reconstructed velocity at t_0 would be in error by as much as 70 m s^{-1} , or 20%. This illustrates the importance of knowing the angle of attack accurately, especially if it exceeds 5° . Note that relative errors in the reconstructed density are twice as large as errors in the reconstructed velocity during the entry phase.

For what concerns the descent phase the sources of errors of the reconstructed trajectory include:

- deviations from hydrostatic equilibrium due to horizontal gradients in the atmosphere;

- measurement errors in PPI, TEM, and GC–MS data;
- errors in correcting pressure and temperature measurements for dynamical effects;
- errors due to neglecting Saturn’s gravitational field and the non-spherically symmetric components of Titan’s gravitational field;
- error in the altitude used at t_0 for the initial condition in the descent phase reconstruction.

We have performed sensitivity tests to study the effects of some of these sources of error on the reconstructed descent trajectory.

Effects of measurements errors on the reconstructed descent trajectory have been investigated through sensitivity tests by comparing the altitude and velocity values estimated at t_1 (time at which we have good quality pressure and temperature data) with the nominal pressure and temperature data. Variations of $\pm 1\sigma$ variations were considered both in pressure (1% of measured value) and temperature data (0.25 K for $T < 105$ and 1.0 K above). While the $\pm 1\sigma$ tests in temperature have a $\pm 1 \text{ km}$ variation in altitude at t_1 , the effect of the $\pm 1\sigma$ in pressure have a variation at t_1 that is less than 20 m confirming that altitude is relatively insensitive to pressure and temperature variation.

For the velocity at t_1 the variation in pressure leads to a change in velocity of around 2.5 m s^{-1} while for temperature this change is less than 0.6 m s^{-1} ; this means that the velocity is poorly sensitive to errors in measured pressure and temperature.

6. Comparison with the official DTWG trajectory

The purpose of the Huygens Descent Trajectory Working Group (DTWG) was to provide a common reference trajectory for the Huygens probe entry and descent trajectory based on all available probe instrument and housekeeping data (Atkinson et al., 2005, 2007). The DTWG considered measurements from the HASI, GC-MS, DWE, SSP, and DISR instruments, from CASU and RASU, and from the probe radar altimeter units (RAU for comparison only). The results of the DTWG trajectory reconstruction effort and the applied methodology is provided by Kazeminejad et al. (2007, 2005) and Kazeminejad and Atkinson (2004). An alternative entry state has been provided by Kazeminejad et al. (2007), which is based on an adjustment of the official Cassini Navigation state vector at 1270 km altitude using a least-squares merging technique that takes into account the state vector and gravitational uncertainties in a 14×14 covariance matrix. The DTWG found that the CNT entry state needed to be adjusted to maximize the consistency of the available data during the Huygens descent phase. The entry altitude of 1270 km was adjusted to 1247.7 km by the DTWG to ensure continuity of altitude at t_0 and impact at 0 km altitude in their reference trajectory. This altitude change was consistent with the uncertainties in the JPL entry state.

This paper presents altitude and velocity at t_0 that are slightly different from DTWG: $\Delta h_{t_0} = 2.3$ km and $\Delta v_{t_0} = 21$ m s⁻¹ which derive essentially by the different entry vector selected. Altitude residuals can be observed in Fig. 15; residuals are significant only in entry phase due to the different merging method; descent phase residuals are well inside the $1-\sigma$ (as calculated from DTWG) and are below 1.5 km.

Velocity residual are instead significant only around t_0 (see Fig. 16), where the merging methods have major differences; it can be seen that after 2000 s residuals are well below 0.4 m s⁻¹.

A bigger discrepancy can be observed in the horizontal motion of the probe and, also in this case, the difference is mainly due to the different entry vector used even if a minor contribution is due to the use of the different model of winds adopted: max Δ long = 0.07° and max Δ lat = 0.1° at t_0 .

Further details on the comparison are given in Aboudan et al. (2008, this issue).

7. Lessons learned

Trajectory of entry probes have been reconstructed from accelerometer data for Venus (Seiff et al., 1980), Mars (Withers et al., 2003), Jupiter, and Titan. Uncertainties in the entry state of Huygens are very large in comparison with previous atmospheric entry missions. They introduce significant uncertainties into the reconstructed trajectory. Future atmospheric probe missions could obtain more

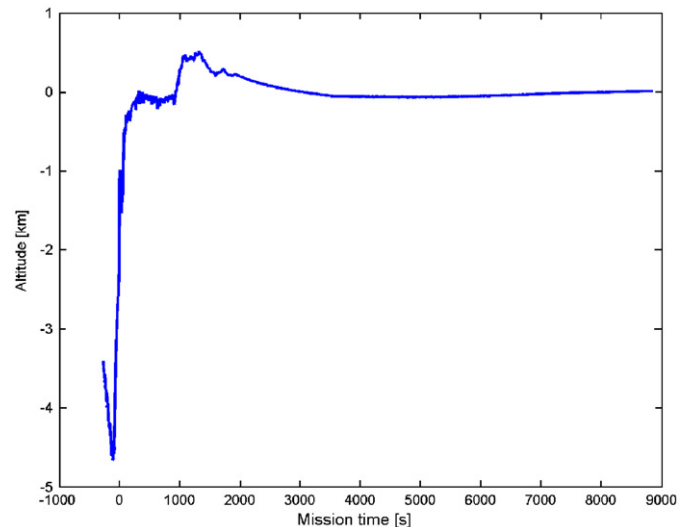


Fig. 15. Altitude residuals (HASI-DTWG). For entry max residual is around 4.7 km at 350 km altitude.

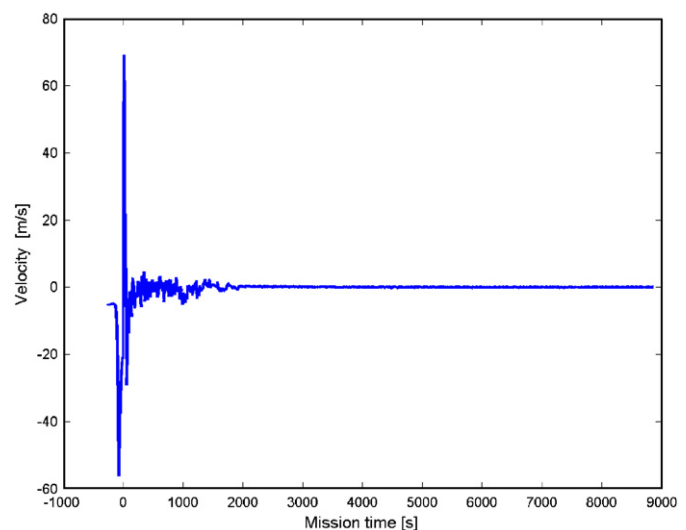


Fig. 16. Velocity residuals (HASI-DTWG). Max residual is around t_0 ; before 2000 s residuals are less than 5 m s⁻¹ and after are well below 0.4 m s⁻¹.

accurate entry states if the probe transmitted radio signals to another spacecraft or to Earth prior to atmospheric entry. The Doppler shift in the received signals would constrain the trajectory of the future probe before atmospheric entry. Future determinations of the altitude of the Huygens landing site will be very useful for reducing the uncertainties in the entry state.

Assumptions about the angle of attack of Huygens also introduce significant uncertainties into the reconstructed trajectory. Future atmospheric probe missions with atmospheric structure experiments should measure spacecraft attitude directly if at all possible. Pre-flight aerodynamic modelling is not yet sufficiently accurate to guarantee that an entry vehicle will have a near-zero angle of attack. The

addition of Yservo and Zservo sensors designed for trajectory reconstruction to the Huygens payload would have increased the accuracy of this work.

On the Huygens probe there were other servo accelerometers (RASU) that have been used for the estimation of the probe spin during descent phase. The measurements of these sensors were recorded during entry but not transmitted via telemetry. These data could have been very useful for the angle of attack determination.

Several other Cassini/Huygens instruments have made or will make measurements that can confirm the validity of this trajectory reconstruction. Cassini RADAR and Cassini RSS will determine the altitude of the Huygens landing site. Zonal winds were derived from the ground-based Doppler data experiment which processed data recorded by the Green Bank and Parkes radio telescopes on Earth that monitored Huygens' signal during the mission. Cassini CIRS measurements of Titan's atmosphere can also be used to infer wind speeds. The Huygens HASI/PWA radar, SSP altimeter, and DISR images can all be used to determine the vertical descent speed of Huygens near impact.

8. Conclusions

The trajectory of the Huygens probe through the atmosphere of Titan on 14 January 2005 has been reconstructed using HASI data. The original entry state of Huygens at the top of Titan's atmosphere has large uncertainties and we have worked to reduce those uncertainties. The quality of data from the ACC Xservo sensor, which measures the axial acceleration, is excellent, but the quality of data from the Ypiezo and Zpiezo sensors, which measure the normal acceleration, is relatively poor. This introduces uncertainties into the derived attitude of the probe during entry, but reconstructed trajectory during the entry phase is relatively insensitive to these uncertainties as long as the actual angle of attack was $\sim 4^\circ$ or less. Data quality during the descent phase is excellent and continuity of results between the entry phase and descent phase is a powerful way to reduce the effects of the large uncertainties in the entry state.

Acknowledgements

HASI has been realized and operated by CISAS under a contract with the Italian Space Agency (ASI), with the participation of RSSD, FMI, IAA, IWF, LPCE and PSSRI sponsored by their respective agencies: ESA, TEKES, CSIC, BM:BWK, CNES, and PPARC. PW acknowledges Michael Mendillo for encouraging this collaboration. We also acknowledge the long years of work by some hundreds of people in the development and design of the Huygens probe. The Huygens probe is part of the Cassini–Huygens mission, a joint endeavour of the National Aeronautics and Space Administration (NASA),

the European Space Agency (ESA) and the Italian Space Agency (ASI).

References

- Aboudan, A., Colombatti, G., Ferri, F., Angrilli, F. 2008. Huygens probe entry trajectory and attitude estimated simultaneously with Titan atmospheric structure by Kalman filtering. *Planet. Space Sci.*, in press, doi:10.1016/j.pss.2007.10.006.
- Angrilli, F., Bianchini, G., Debei, S., Fanti, G., Ferri, F., Fulchignoni, M., Saggin, B., 1996. First results of performance test of temperature sensors of HASI instrument on Cassini/Huygens mission. *Proc. SPIE* 2803, 75–83.
- Atkinson, D.H., Kazeminejad, B., Gaborit, V., Ferri, F., Lebreton, J.-P., 2005. Huygens probe entry and descent trajectory analysis and reconstruction techniques. *Planet. Space Sci.* 53, 586–593.
- Atkinson, D.H., Kazeminejad, B., Lebreton, J.-P., Witasse, O., Pérez-Ayúcar, M., Matson, D.L., 2007. The Huygens probe Descent Trajectory Working Group: Organizational framework, goals, and implementation. *Planet. Space Sci.* 55 (13), 1877–1885.
- Clausen, K.C., Hassan, H., Verdant, M., Couzin, P., Huttin, G., Brisson, M., Sollazzo, C., Lebreton, J.-P., 2002. The Huygens probe system design. *Space Sci. Rev.* 104, 155–189.
- Colombatti, G., Aboudan, A., Ferri, F., Angrilli, F., 2007. Huygens probe entry dynamic model and accelerometer data analysis. *Planet. Space Sci.*, in press, doi:10.1016/j.pss.2007.11.018.
- Doebelin, E.O., 1990. *Measurement Systems: Application and Design*, fourth ed. McGraw-Hill, New York.
- Dougherty, M.K., et al., 2005. Cassini magnetometer observations during Saturn orbit insertion. *Science* 307, 1266–1270.
- Elachi, C., et al., 2005. Cassini Radar views the surface of Titan. *Science* 308, 970–974.
- Flasar, F.M., Allison, M.D., Lunine, J.I., 1997. Titan zonal wind model. In: *Huygens Science, Payload, and Mission*, ESA SP-1177, pp. 287–298.
- Fulchignoni, M., et al., 1997. The Huygens Atmospheric Structure Instrument. In: *Huygens Science, Payload, and Mission*, ESA SP-1177, pp. 163–176.
- Fulchignoni, M., et al., 2002. The characterisation of Titan's atmospheric physical properties by the Huygens Atmospheric Structure Instrument (HASI). *Space Sci. Rev.* 104, 395–431.
- Fulchignoni, M., et al., 2005. In situ measurements of the physical characteristics of Titan's environment. *Nature* 438, 785–791.
- Gaborit, V., 2004. Procedure development for the trajectory reconstruction of a probe descending in a planetary atmosphere: application to Galileo and HASI balloon tests. In: *Planetary Probe Atmospheric Entry and Descent Trajectory Analysis and Science*, ESA SP-544, pp. 151–162.
- Goldstein, H., 1980. *Classical Mechanics*. Addison-Wesley, Reading, MA.
- Harri, A.-M., Fagerström, B., Lehto, A., Leppelmeier, G.W., Mäkinen, T., Pirjola, R., Siikonen, T., Siili, T., 1998. Scientific objectives and implementation of the Pressure Profile Instrument (PPI/HASI) for the Huygens spacecraft. *Planet. Space Sci.* 46, 1383–1392.
- Harri, A.-M., Teemu, M., Asko, L., Henrik, K., Tero, S., 2006. Vertical pressure profile of Titan—observations of the PPI/HASI instrument. *Planet. Space Sci.* 54, 1117–1123.
- Jones, J.C., Giovagnoli, F., 1997. The Huygens probe system design. In: *Huygens Science, Payload, and Mission*, ESA SP-1177, pp. 25–46.
- Kazeminejad, B., Atkinson, D.H., 2004. The ESA Huygens probe entry and descent trajectory reconstruction. In: *Planetary Probe Atmospheric Entry and Descent Trajectory Analysis and Science*, ESA SP-544, pp. 137–149.
- Kazeminejad, B., et al., 2007. Huygens' entry and descent through Titan's atmosphere—methodology and results of the trajectory reconstruction. *Planet. Space Sci.*, doi:10.1016/j.pss.2007.04.013.
- Lebreton, J.-P., Matson, D.L., 1997. The Huygens probe: science, payload and mission overview. In: *Huygens Science, Payload, and Mission*, ESA SP-1177, pp. 5–24.

- Lebreton, J.-P., Matson, D.L., 2002. The Huygens probe: science, payload and mission overview. *Space Sci. Rev.* 104, 59–100.
- Lebreton, J.-P., et al., 2005. Huygens descent and landing on Titan: mission overview and science. *Nature* 438, 758–764.
- Mäkinen, T., 1996. Processing the HASI measurements. *Adv. Space Res.* 17, 219–222.
- Niemann, H.B., et al., 2005. The abundance of constituents of Titan's atmosphere from the GC-MS instrument on the Huygens probe. *Nature* 438, 779–784.
- Ruffino, G., Castelli, A., Coppa, A., Cornaro, C., Foglietta, S., Fulchignoni, M., Gori, F., Salvini, P., 1996. The temperature sensor on the Huygens probe for the Cassini mission: design, manufacture, calibration, and tests of the laboratory prototype. *Planet. Space Sci.* 44, 1149–1162.
- Saggin, B., Angrilli, F., Bianchini, G., Debei, S., Fanti, G., Ferri, F., 1998. Analysis of dynamic performance of HASI temperature sensor during the entry in the Titan atmosphere. *Planet. Space Sci.* 46, 1325–1332.
- Seiff, A., Kirk, D.B., 1977. Structure of the atmosphere of Mars in summer at mid-latitudes. *J. Geophys. Res.* 82, 4364–4378.
- Seiff, A., Kirk, D.B., Young, R.E., Blanchard, R.C., Findlay, J.T., Kelly, G.M., Sommer, S.C., 1980. Measurements of thermal structure and thermal contrasts in the atmosphere of Venus and related dynamical observations: results from the four Pioneer Venus probes. *J. Geophys. Res.* 85, 7903–7933.
- Seiff, A., et al., 1998. Thermal structure of Jupiter's atmosphere near the edge of a 5- μm hot spot in the north equatorial belt. *J. Geophys. Res.* 103, 22857–22889.
- Spencer, D.A., Blanchard, R.C., Braun, R.D., Kallemeyn, P.H., Thurman, S.W., 1999. Mars Pathfinder entry, descent, and landing reconstruction. *J. Spacecraft Rockets* 36, 357–366.
- Strobel, D.F., 2006. Gravitational tidal waves in Titan's upper atmosphere. *Icarus* 182, 251–258.
- Tomasko, M.G., et al., 2005. Rain, winds and haze during the Huygens probe's descent to Titan's surface. *Nature* 438, 765–778.
- Tran, P.S., 2005. Lenoir, Huygens program entry module aerodynamic database/HUY.EADS.MIS.RE.0002. Technical Report, EADS Space Transportation.
- Withers, P., 2006. Spirit and opportunity trajectory and atmospheric structure reconstruction. *Icarus* 185, 133–142.
- Withers, P., Towner, M.C., Hathi, B., Zarnecki, J.C., 2003. Analysis of entry accelerometer data: a case study of Mars Pathfinder. *Planet. Space Sci.* 51, 541–561.
- Withers, P., Towner, M.C., Hathi, B., Zarnecki, J.C., 2004. Review of the trajectory and atmospheric structure reconstruction for Mars Pathfinder. In: *Planetary Probe Atmospheric Entry and Descent Trajectory Analysis and Science*, ESA SP-544, pp. 163–174.
- Yelle, R.V., 2004. Titan Atmospheric Model Working Group Internal Report.
- Zarnecki, J.C., Ferri, F., Hathi, B., Leese, M.R., Ball, A.J., Colombatti, G., Fulchignoni, M., 2004. In-flight performance of the HASI servo accelerometer and implications for results at Titan. In: *Planetary Probe Atmospheric Entry and Descent Trajectory Analysis and Science*, ESA SP-544, pp. 71–76.
- Zarnecki, J.C., et al., 2005. A soft solid surface on Titan as revealed by the Huygens Surface Science Package. *Nature* 438, 792–795.